^{19}Ne levels studied with the ^{18}F(d, n)^{19}Ne*(^{18}F+p) reaction

A. S. Adekola,[1,2,*] C. R. Brune,[1] D. W. Bardayan,[3] J. C. Blackmon,[3,†] K. Y. Chae,[4,5] J. A. Cizewski,[2] K. L. Jones,[2,‡] R. L. Kozub,[6] T. N. Massey,[1] C. D. Nesaraja,[3] S. D. Pain,[2,§] J. F. Shriner Jr.,[6] M. S. Smith,[3] and J. S. Thomas[2,‖]

[1]*Department of Physics and Astronomy, Ohio University, Athens, Ohio 45701, USA*

[2]*Department of Physics and Astronomy, Rutgers University, Piscataway, New Jersey 08854, USA*

[3]*Physics Division, Oak Ridge National Laboratory, Oak Ridge, Tennessee 37831, USA*

[4]*Department of Physics and Astronomy, University of Tennessee, Knoxville, Tennessee 37996, USA*

[5]*Department of Physics, Sungkyunkwan University, Suwon 440-746, Korea*

[6]*Department of Physics, Tennessee Technological University, Cookeville, Tennessee 38505, USA*

(Received 23 January 2012; published 9 March 2012)

A good understanding of the level structure of ^{19}Ne around the proton threshold is critical to estimating the destruction of long-lived ^{18}F in novae. Here we report the properties of levels in ^{19}Ne in the excitation energy range of $6.9 \leqslant E_x \leqslant 8.4$ MeV studied via the proton-transfer ^{18}F(d, n)Ne* reaction at the Holifield Radioactive Ion Beam Facility. The populated ^{19}Ne levels decay by breakup into $p + {}^{18}$F and $\alpha + {}^{15}$O particles. The results presented in this manuscript are those of levels that are simultaneously observed from the breakup into both channels. An s-wave state is observed at 1468 keV above the proton threshold, which is a potential candidate for a predicted broad $J^\pi = 1/2^+$ state. The proton and α partial widths are deduced to be $\Gamma_p = 228 \pm 50$ keV and $\Gamma_\alpha = 130 \pm 30$ keV for this state.

DOI: 10.1103/PhysRevC.85.037601 PACS number(s): 27.20.+n, 25.40.Hs, 25.60.−t, 26.30.−k

Knowledge of the properties of resonances near the proton threshold in ^{19}Ne is required to determine the ^{18}F$(p, \alpha)^{15}$O reaction rate, which predominantly destroys the long-lived radionuclide ^{18}F in nova outbursts. The reaction rate is dominated by s- and p-wave resonances in ^{19}Ne arising from states near the proton threshold at 6411 keV. Despite years of measurements with stable and radioactive beams to better understand this reaction [1–9], the cross section has only been measured directly down to ∼250 keV [10]. Large uncertainties remain due to the unknown properties of levels near the proton threshold and unknown characteristics of the interference between the $J^\pi = 3/2^+$ resonances.

The present understanding is that the ^{18}F$(p, \alpha)^{15}$O rate is dominated by the two known resonances at $E_{\text{c.m.}} = 665$ keV ($J^\pi = 3/2^+$) and 330 keV ($J^\pi = 3/2^-$) that arise from ^{19}Ne levels at $E_x = 7076$ and 6741 keV, respectively [11,12]. Dufour and Descouvemont [13] predict an s-wave state around 1.5 MeV above the proton threshold with decay widths of $\Gamma_p = 157$ keV and $\Gamma_\alpha = 139$ keV; that such a state has yet to be confirmed supports the need for additional studies of the level structure of ^{19}Ne. A tentative observation of a broad state near this energy was measured by Dalouzy *et al.* [14] using the inelastic scattering reaction ^{1}H(^{19}Ne, p)^{19}Ne*(p)^{18}F, but the proton and α widths could not be determined.

The ^{18}F(d, n) reaction had been previously studied at the Oak Ridge National Laboratory (ORNL) Holifield Radioactive Ion Beam Facility (HRIBF) in order to clarify the level structure of ^{19}Ne near the proton threshold. The final ^{19}Ne states at these excitation energies decay promptly into $\alpha + {}^{15}$O particles. However, at higher excitation energies, the states become broader, and breakup into the $p + {}^{18}$F channel becomes stronger. The present experimental approach of using the proton-transfer reaction ^{18}F(d, n) enables the study of resonances that have a yield too small to be measured directly in the ^{18}F(p, α) reaction. In addition, since both sets of decay products were detected in coincidence by silicon detectors, the decay branching ratios can be determined from

$$\frac{\Gamma_p}{\Gamma_\alpha} = \frac{N_p}{N_\alpha}\frac{\epsilon_\alpha}{\epsilon_p}, \tag{1}$$

where $\Gamma_{p,\alpha}$, $N_{p,\alpha}$, and $\epsilon_{p,\alpha}$ are the partial widths, coincidence yield, and detection efficiency, respectively, for the breakup of ^{19}Ne states into the p and α channels.

The results from the breakup of ^{19}Ne to $\alpha + {}^{15}$O particles focusing on levels close to the proton threshold have been previously published [15,16]. This Brief Report presents analysis of states in ^{19}Ne that appear in both p- and α-decay channels in the excitation energy range of $6.9 \leqslant E_x \leqslant 8.4$ MeV that corresponds to ∼0.5–2.0 MeV above the proton threshold. Spectroscopic factors were extracted for strongly populated levels from which proton widths could be deduced. The α widths were then estimated from the observed proton to α branching ratios.

The detailed description of the experimental approach is in Refs. [15,16]. The measurements of the ^{18}F(d, n) reaction were performed at ORNL's HRIBF utilizing a 150-MeV isotopically pure ^{18}F beam to bombard a 716-μg/cm^2 CD_2 target. The reaction neutrons were emitted predominantly at

*aderemi.ade@gmail.com

†Present address: Department of Physics and Astronomy, Louisiana State University, Baton Rouge, Louisiana 70803 USA.

‡Present address: Department of Physics and Astronomy, University of Tennessee, Knoxville, Tennessee 37996, USA.

§Present address: Physics Division, Oak Ridge National Laboratory, Oak Ridge, Tennessee 37831, USA.

‖Present address: School of Electronics and Physical Sciences, University of Surrey, Guildford, Surrey GU2 7XH, United Kingdom.

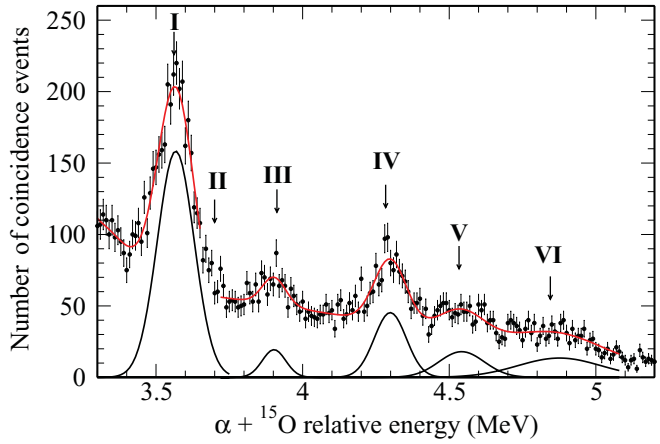

FIG. 1. (Color online) Partial spectrum from the breakup of ^{19}Ne $\rightarrow \alpha + {}^{15}$O above 3.3 MeV of $\alpha + {}^{15}$O relative energy. The fits are to the five resolved levels (I and III–VI). The red line is the sum of the individual peaks shown as black solid lines. State IV is the state of interest in the proton channel.

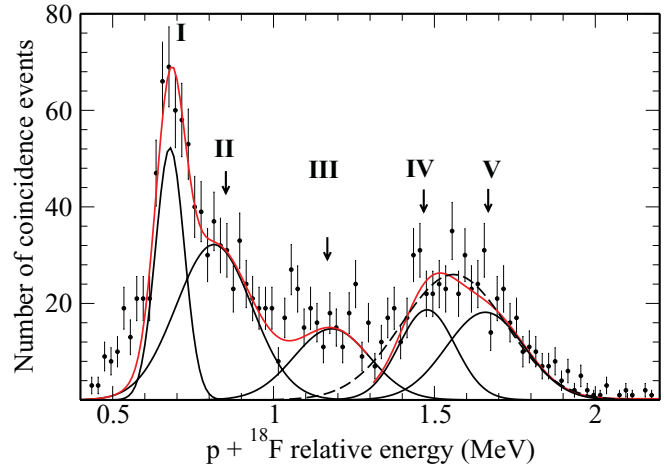

FIG. 2. (Color online) Spectrum from the breakup of ^{19}Ne $\rightarrow$ $p + {}^{18}$F with fits to the five levels (I–V). The red line is the sum of the individual peaks shown as black solid lines. The excitation energies determined for ^{19}Ne are listed in Table I.

backward angles in the laboratory system while the ^{19}Ne was limited to a narrow cone at forward angles. The neutrons were not measured. The ^{19}Ne states near the proton threshold decay promptly by emitting α particles. However, at higher excitation energies, the states become broader, and decay via proton emission becomes stronger. Each pair of charged particle decay products was detected in coincidence using six 5-cm × 5-cm position-sensitive E-ΔE telescopes located ≈46 cm downstream of the target, allowing for the measurement of energy, position, and particle type. Two of the telescopes covered laboratory angles 2.5°–8.5° on both sides of the beam axis and were optimized to measure heavier particles. The remaining four telescopes covered laboratory angles 10.5°–16.5° on both sides of the beam axis and were optimized to detect the light particles.

The ^{18}F(d, n) reaction populates excitations in ^{19}Ne above the α-particle unbound region. Therefore the residual ^{19}Ne was observed in its breakup channels. The $\alpha + {}^{15}$O relative energy spectrum obtained [15,16] using the coincidence, particle identification, and Q-value requirements is shown in Fig. 1. The $p + {}^{18}$F relative energy spectrum is shown in Fig. 2. The proton breakup spectrum was analyzed with the MINUIT [17] fitting program using five Gaussian peaks covering $6.9 \leqslant E_x \leqslant 8.4$ MeV. These peaks correspond to excited states in ^{19}Ne that have relatively large branching ratios for proton emission. The parameters extracted from the fit are presented in Table I. The fitting was done while allowing the area, resonance energy, and width to vary as free parameters.

Figure 3 shows the expected full width at half maximum (FWHM) resolution of the reconstructed relative energy $E_{\rm rel}$ as a function of $E_{\rm rel}$ in the p channel calculated from a Monte Carlo simulation. Also shown in Fig. 3 are the measured resolutions of the individual peaks identified in Fig. 2. There is reasonably good agreement between the calculated and experimentally measured resolution for peaks I, IV, and V. The measured width of peaks II and III exceeded the experimental resolution. The intrinsic width of the state might be large, or it could be that the peaks consist of two or more unresolved states.

Decay branching ratios were determined for states that appear in both α- and p-decay channels using Eq. (1). The coincidence efficiencies ϵ_p and ϵ_α were calculated as a function of center-of-mass angle for each excitation energy with the Monte Carlo simulation assuming that the decay is isotropic in the center-of-mass system. The resulting $p + {}^{18}$F coincidence efficiency, integrated over the acceptance of the present experiment, is shown as a function of relative energy in Fig. 4. Because of the detector thicknesses used in the experiment, the energy range of protons that could be stopped and identified in the telescopes was from 4 to 12 MeV. This energy acceptance range in part determines the acceptance of the experiment and explains the observed low-energy and high-energy falloffs in the measured relative energy spectra

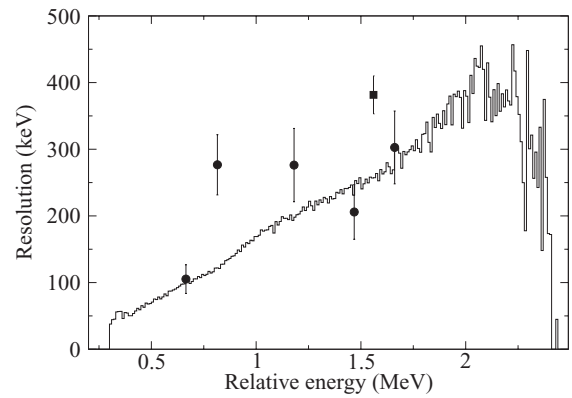

FIG. 3. The Monte Carlo simulated (solid histogram) FWHM resolution for the reconstructed relative energy for $p + {}^{18}$F. The observed experimental resolutions are indicated by solid circles. The square data point is the resolution that the peak at $E_{\rm c.m.} = 1.5$ MeV would have when fitted with only one peak.

TABLE I. Resonance parameters of levels in ^{19}Ne measured from the ^{18}F$(d,n)^{19}$Ne$^*(p+^{18}$F) reaction. Except where indicated, known resonance energies were taken from Ref. [18], and their decay branching ratios were calculated using the widths adopted from the same reference.

	This experiment				Previous works			
	E_r (keV)	E_x (keV)	Γ_p (keV)	Γ_p/Γ_α	E_r (keV)	E_x (keV)	Γ_p (keV)	Γ_p/Γ_α
I	678(5)	7089(5)	13.5(7)[a]	0.64(4)	665	7076	15.2(1.0)	0.639(66)
II	815(20)	7226(20)			827	7238		0.058
III	1181(15)	7592(15)						
IV	1468(26)	7879(26)	228(50)	1.754(14)	1452(39)[b]	7863(39)[c]	$\Gamma = 292(107)$[d]	1.129[e]
V	1661(30)	8072(30)	3.34(2.89)	15.2(1.2)	1658	8069		

[a]Taken from Ref. [16].
[b]Reference [14].
[c]Reference [14].
[d]The total width Γ taken from Ref. [14].
[e]Γ_p and Γ_α are theoretical values from Ref. [13].

(see Fig. 2). The analogous plot for the $\alpha + ^{15}$O channel was published in Ref. [16].

The peak labeled I in Fig. 2 is centered at $E_x = 7089$ keV, which agrees with the extracted centroid from the α data. This energy corresponds to the well-known state at $E_x = 7076$ keV. In addition to the relatively good agreement in excitation energy, the extracted branching ratio $\Gamma_p/\Gamma_\alpha = 0.64 \pm 0.04$ is in excellent agreement with the value of 0.639 ± 0.066 determined from previous widths of $\Gamma_p = 15.2 \pm 1.0$ keV and $\Gamma_\alpha = 23.8 \pm 0.12$ keV [12].

The peak labeled II is measured at $E_x = 7266 \pm 20$ keV; this may correspond to the known state at $E_x = 7238$ keV. A careful look at the α data (Fig. 1) reveals a high-energy tail on the 7089-keV state that might be an indication of this state.

As for the peak labeled III, the statistics were too poor to reach firm conclusions. Although an excitation energy of $E_x = 7592$ keV was deduced by assuming only one state in the fit, the poor-quality data would also be consistent with more than one state in this excitation energy region.

The peak at $E_{\text{c.m.}} = \sim 1.5$ MeV in Fig. 2 also seems to be too broad to consists of a single state. A fit to this peak with one Gaussian function is shown as the black dashed line, giving a measured width of ~400 keV, shown as the square in Fig. 3.

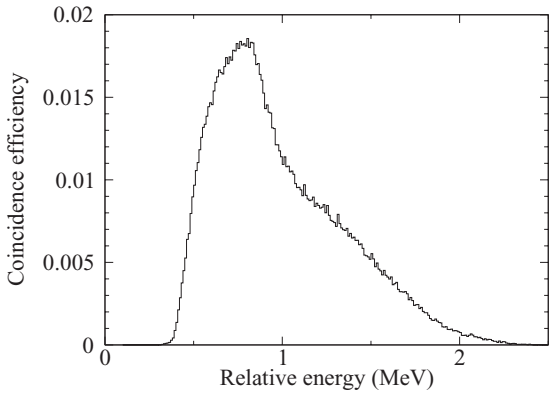

FIG. 4. The calculated $p + ^{18}$F coincidence efficiency for geometry used in this measurement.

Such a large width could reflect unresolved peaks. The red line in Fig. 2 corresponds to the best fit in this energy region assuming two levels are being populated. The best fit is shown as peaks labeled IV and V with energies at $E_x = 7879 \pm 26$ and 8072 ± 30 keV, which correspond to states that appear at $E_x = 7834 \pm 6$ and 8081 ± 10 keV in the α data shown in Fig. 1.

The peak labeled V measured at $E_x = 8072$ keV is likely the known state at $E_x = 8069$ keV. The Γ_p for this level is unknown, while the known Γ_α is 0.22 ± 0.19 keV [18]. In this work, the decay branching determined for this state was $\Gamma_p/\Gamma_\alpha = 15.2 \pm 1.2$, translating into $\Gamma_p = 3.34 \pm 2.89$ keV. The errors on all the quantities presented in this manuscript are statistical. Sources of systematics errors and their contributions are given in Ref. [16].

Unfortunately, the limited statistics prevent extraction of meaningful neutron angular distributions from the ^{18}F$(d,n)^{19}$Ne$^*(p + ^{18}$F) reaction. However, the neutron angular distributions extracted for the 7834-keV state from the α-decay channel can be normalized to obtain differential cross sections using Eq. (7) of Ref. [16] and is shown in Fig. 5. The

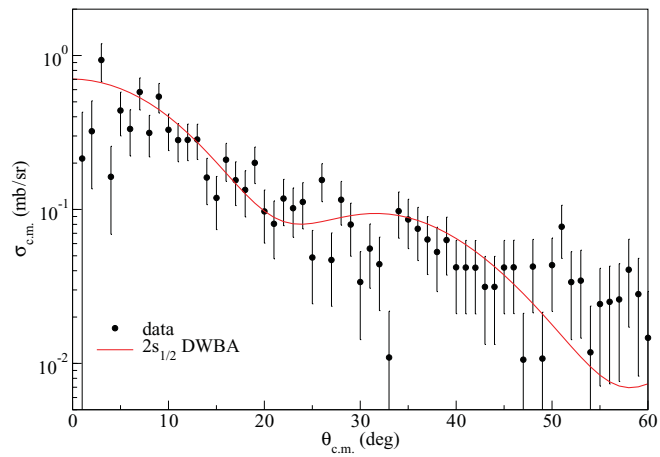

FIG. 5. (Color online) The differential cross sections for (d,n) transfer to the 7834-keV state in ^{19}Ne. These data are deduced from the α-decay channel.

differential cross sections were compared to distorted-wave Born approximation (DWBA) calculations to extract spectroscopic factors. A DWBA calculation with angular momentum transfer $\ell = 0$ well reproduces the angular distributions. The J^π of this state could be $1/2^+$ or $3/2^+$ since the J^π of $^{18}\mathrm{F}_{\mathrm{g.s.}}$ is 1^+. The spectroscopic factor extracted for this state is $(2J+1)S_p = 0.25 \pm 0.05$ assuming $J^\pi = 1/2^+$. The decay branching ratio Γ_p/Γ_α of 1.754 ± 0.014 measured for this state allowed for determination of p- and α-decay branching ratios of 0.637 ± 0.005 and 0.363 ± 0.003, respectively, assuming negligible γ width and isotropic angular distributions. Using the measured spectroscopic factor, a partial proton width of $\Gamma_p = 228 \pm 50$ keV was determined using the same procedure described previously [15], and a partial α width of $\Gamma_\alpha = 130 \pm 30$ keV was extracted using the decay branching ratio for this state. The energy and the estimated widths of this resonance are consistent with the prediction of an s-wave state around 1.5 MeV above the proton threshold by Dufour and Descouvemont [13].

In summary, the proton-transfer reaction $^{18}\mathrm{F}(d,n)$ was used to populate states in $^{19}\mathrm{Ne}$ at excitation energies around 1.5 MeV above the proton threshold. The populated states decay by breakup into $p + {}^{18}\mathrm{F}$ and $\alpha + {}^{15}\mathrm{O}$ particles. The detection of both decay products in coincidence allowed for direct determinations of decay branching ratios Γ_p/Γ_α. The decay branching ratio of the known resonance at $E_{\mathrm{c.m}} = 665$ keV was consistent with previous measurements. The spin and widths determined for an observed resonance at 1468 keV are consistent with the prediction of Dufour and Descouvemont [13] of an s-wave state with excitation energy at $\sim$1.5 MeV above proton threshold.

This work was supported in part by the US Department of Energy under Grants No. DEFG02-88ER40387 (Ohio University), No. DE-FG02-96ER40990 and No. DE-FG02-96ER40955 (Tennessee Technical University) and the National Nuclear Security Administration under the Stewardship Science Academic Alliances program through US Department of Energy Cooperative Agreement No. DE-FG52-08NA28552 and the National Science Foundation (RUTGERS).

[1] H. T. Fortune, A. Lacaze, and R. Sherr, Phys. Rev. C **82**, 034312 (2010).
[2] H. T. Fortune and R. Sherr, Phys. Rev. C **73**, 024302 (2006).
[3] H. T. Fortune and R. Sherr, Phys. Rev. C **61**, 024313 (2000).
[4] R. Coszach, M. Cogneau, C. R. Bain, F. Binon, T. Davidson, P. Decrock, T. Delbar, M. Gaelens, W. Galster, J. S. G. J. Görres *et al.*, Phys. Lett. B **353**, 184 (1995).
[5] Y. M. Butt, J. W. Hammer, M. Jaeger, R. Kunz, A. Mayer, P. D. Parker, R. Schreiter, and G. Staudt, Phys. Rev. C **58**, R10 (1998).
[6] A. St. J. Murphy, A. M. Laird, C. Angulo, L. Buchmann, T. Davinson, P. Descouvemont, S. P. Fox, J. José, R. Lewis, C. Ruiz *et al.*, Phys. Rev. C **79**, 058801 (2009).
[7] D. W. Visser, J. A. Caggiano, R. Lewis, W. B. Handler, A. Parikh, and P. D. Parker, Phys. Rev. C **69**, 048801 (2004).
[8] D. W. Bardayan, J. C. Blackmon, J. Gomez del Campo, R. L. Kozub, J. F. Liang, Z. Ma, L. Sahin, D. Shapira, and M. S. Smith, Phys. Rev. C **70**, 015804 (2004).
[9] J.-S. Graulich, S. Cherubini, R. Coszach, S. El Hajjami, W. Galster, P. Leleux, W. Bradfield-Smith, T. Davinson, A. Di Pietro, A. C. Shotter *et al.*, Phys. Rev. C **63**, 011302 (2000).
[10] C. E. Beer, A. M. Laird, A. S. J. Murphy, M. A. Bentley, L. Buchman, B. Davids, T. Davinson, C. A. Diget, S. P. Fox, B. R. Fulton *et al.*, Phys. Rev. C **83**, 042801 (2011).
[11] D. W. Bardayan, J. C. Blackmon, W. Bradfield-Smith, C. R. Brune, A. E. Champagne, T. Davinson, B. A. Johnson, R. L. Kozub, C. S. Lee, R. Lewis *et al.*, Phys. Rev. C **63**, 065802 (2001).
[12] D. W. Bardayan, J. C. Batchelder, J. C. Blackmon, A. E. Champagne, T. Davinson, R. Fitzgerald, W. R. Hix, C. Iliadis, R. L. Kozub, Z. Ma *et al.*, Phys. Rev. Lett. **89**, 262501 (2002).
[13] M. Dufour and P. Descouvemont, Nucl. Phys. A **785**, 381 (2007).
[14] J. C. Dalouzy *et al.*, Phys. Rev. Lett. **102**, 162503 (2009).
[15] A. S. Adekola, D. W. Bardayan, J. C. Blackmon, C. R. Brune, K. Y. Chae, C. Domizioli, U. Greife, Z. Heinen, M. J. Hornish, K. L. Jones *et al.*, Phys. Rev. C **83**, 052801(R) (2011).
[16] A. S. Adekola, D. W. Bardayan, J. C. Blackmon, C. R. Brune, K. Y. Chae, C. Domizioli, U. Greife, Z. Heinen, M. J. Hornish, K. L. Jones *et al.*, Phys. Rev. C **84**, 054611 (2011).
[17] MINUIT-Function Minimization and Error Analysis, CERN Program Library Long Writeup D506, 1994.
[18] C. D. Nesaraja, N. Shu, D. W. Bardayan, J. C. Blackmon, Y. S. Chen, R. L. Kozub, and M. S. Smith, Phys. Rev. C **75**, 055809 (2007).